Supporting Information

3D structure aerogels constructed by reduced graphene oxide and hollow TiO_2 spheres for efficient visible-light-driven photoreduction of U(VI) in air-equilibrated wastewater

Zhimin Dong[a], Zhibin Zhang[a,b*], Zifan Li[a], Yue Feng[c], Wenjie Dong[a], Ting Wang[a], Zhongping Cheng[a], Youqun Wang[a], Ying Dai[a], Xiaohong Cao[a], Yuhui Liu[a], Yunhai Liu[a,b*]

[a]*State Key Laboratory of Nuclear Resources and Environment, East China University of Technology, Nanchang, Jiangxi 330013, P.R. China*

[b]*Jiangxi Province Key Laboratory of Synthetic Chemistry, East China University of Technology, Nanchang, Jiangxi 330013, China*

[c]*Department of architectural design, Nuclear Power Institute of China, Chengdu, Sichuan 610213, China*

***Corresponding Authors:** E-mail: yhliu@ecut.edu.cn (Y.H. Liu), zhbzhang@ecut.edu.cn (Z.B. Zhang).

S1 Chemicals

Tetrabutyltitanate (TBT), acetonitrile (C_2H_3N), ammonia (NH_4OH, 25-28 wt%), t-BuOH (TBA) and p-benzoquinone (BQ) were purchased from Aladdin Chemistry Co. Ltd. And the radicals were trapped with 5,5-Dimethyl-1-pyrroline-N-oxide (DMPO) obtained from TCL. graphene oxide (GO) was purchased from XFNANO. The uranium solution used in the experiment is obtained by dissolving $UO_2(NO_3)_2$□$6H_2O$ in mixture of deionized water and methanol (V_w/V_m=19:1).

S2 Preparation of the TiO_2 hollow sphere

Typically, 79 mL of ethanol, 3.9 mL of ammonia, and 1.4 mL of water were mixed with 1.0 g of SiO_2 nanospheres to obtain SiO_2 dispersion solution. Then, 28 mL of acetonitrile was added to the SiO_2 dispersion with stirring for obtaining dispersion A. The dispersion B was prepared by mixing 36 mL of ethanol, 12 mL of acetonitrile with 2 mL of TBT. Subsequently, the dispersion B was added to the dispersions A drop by drop. The mixture was vigorously stirred for 12 h. The obtained white suspension was separated by centrifuged, and was washed with ethanol three times and dried in oven at 80 °C form $SiO_2@TiO_2$ nanospheres precursor. The core-shell $SiO_2@TiO_2$ nanospheres were obtained by sintering $SiO_2@TiO_2$ nanospheres precursor under air to 500 °C at 1 °C $\cdot$min^{-1} ramp for 3 h.

The SiO_2@TiO_2 nanospheres were dispersed in 35 mL of 2.00 mol·L^{-1} NaOH solution, and then was transferred to 50 mL Teflon-sealed autoclave and maintained at 80 °C for 4 h. The resulting products were washed with water until neutrality and dried at 60 °C under vacuum overnight to obtain the hollow TiO_2 sphere (H-TiO_2).

S3 Characterization

The distribution, size, and morphology of the as-prepared samples were characterized by scanning electron microscopy (SEM) (Hitachi S-4800 FESEM), TEM (JEOL, Japan), nitrogen adsorption-desorption measurements (Micromeritics ASAP 2020). The crystal structure of the products was characterized by X-ray diffraction (XRD, Bruker D8 Advance diffractometer) within 2θ range from 5° to 80° with Cu Kα radiation ($\lambda = 0.15418$ nm) at a scan rate of 0.05°·s^{-1}. The Raman spectra were observed on a spectroscopy (DXR spectrophotometer, Thermo Fisher Scientific, USA) under laser light (λ=532 nm). The structure of the compound was further confirmed by Fourier-transform infrared spectroscopy (Nicolet 6700, Thermo, USA) at the wavelength of 4000-500 cm^{-1}. SDT Q600 thermal analyzer (TA instruments) was used to obtain thermogravimetric (TG) and differential thermogravimetric (DTG) curves. The experiments were performed in a helium or in air atmosphere from a room temperature up to 800 °C (heating rate of 5 °C·min^{-1}). meter with a Mg Ka X-ray source (1,253.5 eV photons). The zeta potential values of samples suspensions were measured by a Brookhaven Zeta Plus zeta potential analyzer. The valence state and surface energy state distribution of photocatalysts were obtained using XPS (Escalab 250Xi, Thermo Fisher Scientific, USA). The UV-Vis Diffuse Reflectance Spectroscopy (UV-Vis DRS) was tested on a Hitachi U-300 with a scanning range of 200-800 nm and a white standard of $BaSO_4$ was used as a reference. The energy band gap (E_g) of the as-synthesized photocatalysts was calculated according to the UV–vis absorption spectra. In semiconductor physics, the formula $(\alpha h\upsilon)^m = A(h\upsilon - E_g)$ was used to relate the absorption coefficient to the energy band gap, where α, h, υ, A and E_g corresponded to the absorption coefficient, Planck constant, light vibration frequency, proportional constant and band gap energy, respectively. The m value depended on the nature of the electronic transition, when m=0.5, the TiO_2 semiconductor had an indirect band gap. The time-resolved photoluminescence (PL) decay curves were measured by an FLS920 fluorescence lifetime spectrophotometer (Edinbergh instrument, UK) under 360 nm light excitation. The time-resolved PL spectra decay curves were fitted by the following multiexponential equation.

$$I = I_O t^{\beta-1} \exp\left\{ -\left(\frac{t}{\tau} \right)^{\beta} \right\} \tag{1}$$

The average lifetime of two exponential decay is essential to describe the overall TRPL character, which is calculated using Eq.

$$\tau = \sum_{i=1,2} B_i \tau_i^2 / \sum_{i=1,2} B_i \tau_i \tag{2}$$

where l is the average lifetime, B_i and τ_i are the amplitude (preexponential factor) and the PL decay time of the individual components, respectively.

S4 The calculation of charge diffusion length

Difference of lifetime between electrons and holes is neglected to simplify the calculation as adopted in previous studies, where the nominal diffusion length provides a comparative assessment of bulk recombination. The charge diffusion lengths (L) are calculated by the follow equations:

$$L = \sqrt{D\tau} \tag{3}$$

$$\mu = \frac{qD}{k_B T} \tag{4}$$

where L is the nominal diffusion length, D is the diffusion coefficient and τ is the lifetime of charges, q, k_B and T represent elementary charge, Boltzmann constant and Kelvin temperature, respectively, μ is mobility of charges (1.0 or 0.3 $cm^2 \cdot V^{-1} \cdot S^{-1}$ for electrones or holes in TiO_2).

S5 Photoelectrochemical Tests

Electrochemical measurements were carried out on a CHI660E electrochemical workstation (Shanghai Chenhua, China) using a conventional three electrode cell with a Pt plate as the counter electrode, Ag/AgCl electrode as the reference electrode and working electrodes prepared with samples have an active area of 1 cm^2. Electrochemical impedance spectroscopy (EIS) measurement was carried out on a CHI660C electrochemical analyzer in 25 $mmol \cdot L^{-1}$ $K_3[Fe(CN)_6]$ solution with an alternating current signal (10 mV) in the frequency range of 0.1-10^5 Hz at open circuit potential. Mott-Schottky plots were recorded on the above mentioned three electrode system by using the Impedance-Potential technique in Na_2SO_4 aqueous solution (0.5 $mol \cdot L^{-1}$). With reference to the Mott-Schottky plots, the flat-band potentials of samples can be calculated according to the conversion formula: *E*(RHE) =

E(Ag/AgCl) + E^{θ} + 0.059 pH (2), where E^{θ} (Ag/AgCl) = 0.197 V.

S6 Photocatalytic test

The batch experiment of photocatalytic reduction of U(VI) was performed in a Pyrex top-irradiation reaction vessel. Specifically, 10 mg 3D RGO@TiO$_2$-x samples were added into 100 mL solutions containing 50 mg·L^{-1} U(VI) and various concentrations of NaCl (0.01 mol·L^{-1}, 0.1 mol·L^{-1}, 0.25 mol·L^{-1}, and 0.50 mol·L^{-1}) at different pH (4.0, 5.0, 6.0, and 7.0), and the mixture was stirred continuously. The pH value of the suspension was then adjusted with a small amount of 1 mol·L^{-1}, 0.1 mol·L^{-1} and 0.01 mol·L^{-1} HNO$_3$ or Na$_2$CO$_3$ solutions, and the impact of the pH regulation solutions could be ignored. A 300 W Xe lamp equipped with an ultraviolet cutoff filter ($\lambda \geq 420$ nm) was utilized as the visible light source. Before irradiation, the mixed solution was magnetically stirred in the dark for 2 h so that it reached the adsorption-desorption equilibrium. After illumination for a certain time, the absorbance of UO$_2^{2+}$ at a wavelength of 650 nm was analyzed by a UV-vis spectrophotometer using Arsenazo III spectrophotometric method. The reduction ratio of UO$_2^{2+}$ was calculated as C_e/C_o, where C_o and C_e are the initial and final concentrations of uranium (mg·L^{-1}) at different time. All samples were isolated by filtration for further analysis.

S7 Trapping Experiment

For radical trapping experiments, the scavenger for each reactive species was added to the reaction solution in a manner similar to that described for the photocatalytic experiment (above). In these experiments, we used p-benzoquinone (BQ, 1 mmol·L^{-1}), t-BuOH (TBA, 1 mmol·L^{-1}), and CH$_3$OH (5 vol %) as ·O$_2^-$, ·OH, electron, and h$^+$ scavengers, respectively. In each experiment, 10 mg of 3D RGO@TiO$_2$-3 was added to an aqueous U(VI) solution (100 mL, 50 mg·L^{-1}), and the mixture was magnetically stirred for 60 min in the dark to achieve high dispersion and adsorption-desorption equilibrium between the U(VI) and 3D RGO@TiO$_2$-3. Then, positioned 350 mm away from the visible light source. Samples were collected after for a certain time of irradiation, and then filtration through a 0.22 μm PES membrane to remove the 3D RGO@TiO$_2$-3. The concentration of the remaining U(VI) concentration was monitored by measuring the absorbance of the solution at 650 nm. For comparison, control experiments were performed using 3D RGO@TiO$_2$-3 as a catalyst, or without any photocatalyst, under the same conditions.

The detection of hydroxyl radicals by spin trapping electron paramagnetic resonance (EPR) were carried out at a Bruker model A300 spectrometer. The EPR experiment was primarily focused on the analysis of$\cdot O_2^-$. In the case of O_2^-, the whole test was performed in aqueous solution. First, 5 mg of sample was weighed and dispersed in 5 mL methanol via ultrasound for 20 min; then, DMPO (100 mmol·L^{-1}) solution was used for hybrid acquisition under visible light.

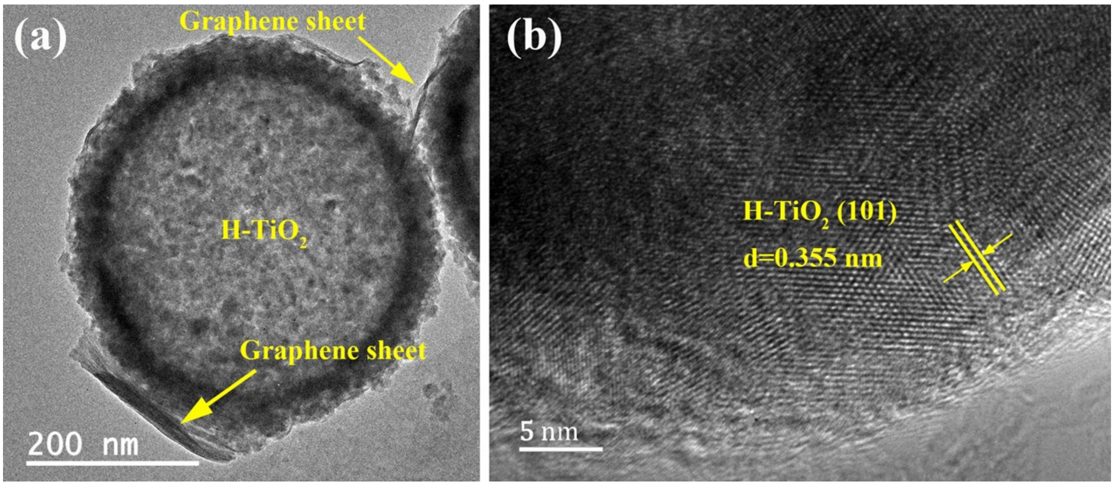

Figure S1 (a) TEM and (b) HRTEM images of the 3D RGO@TiO_2-3 composite

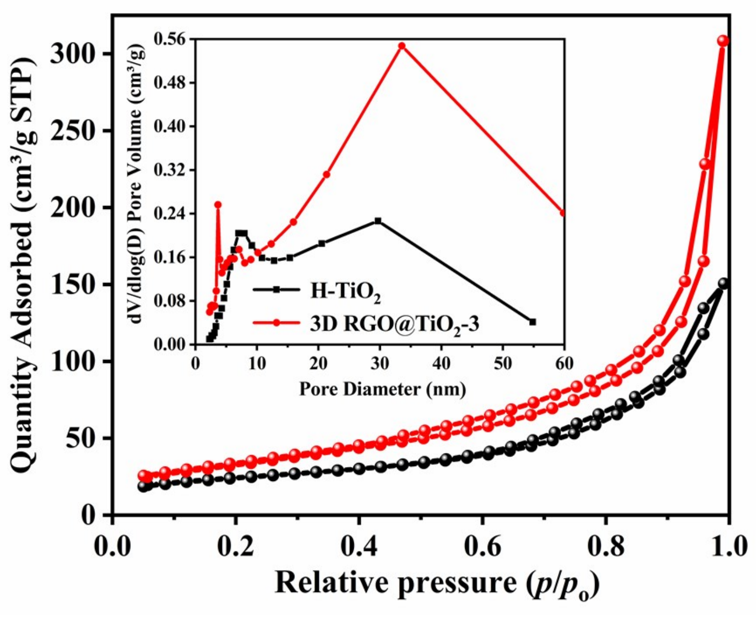

Figure S2 N_2 adsorption-desorption isotherms and the corresponding pore size distribution curves (insets) of the H-TiO_2 and 3D RGO@TiO_2-3

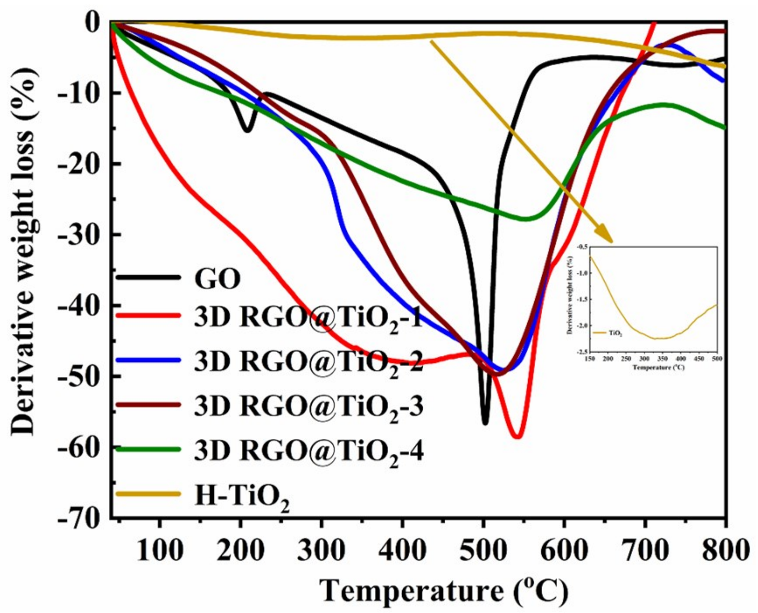

Figure S3 The differential thermogravimetric curves in air.

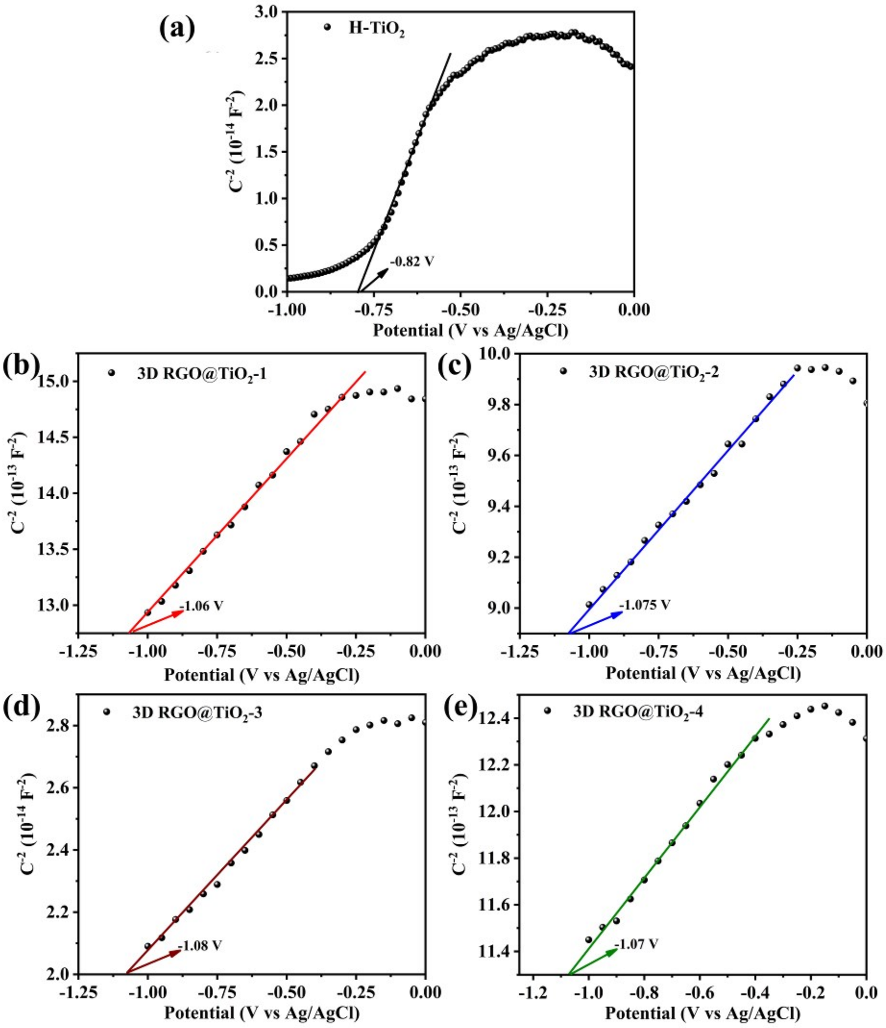

Figure S4 Mott-Schottky plots of H-TiO_2 (a), 3D RGO@TiO_2-1 (b), 3D RGO@TiO_2-2(c), 3D RGO@TiO_2-3 (d) and 3D RGO@TiO_2-4 (e).

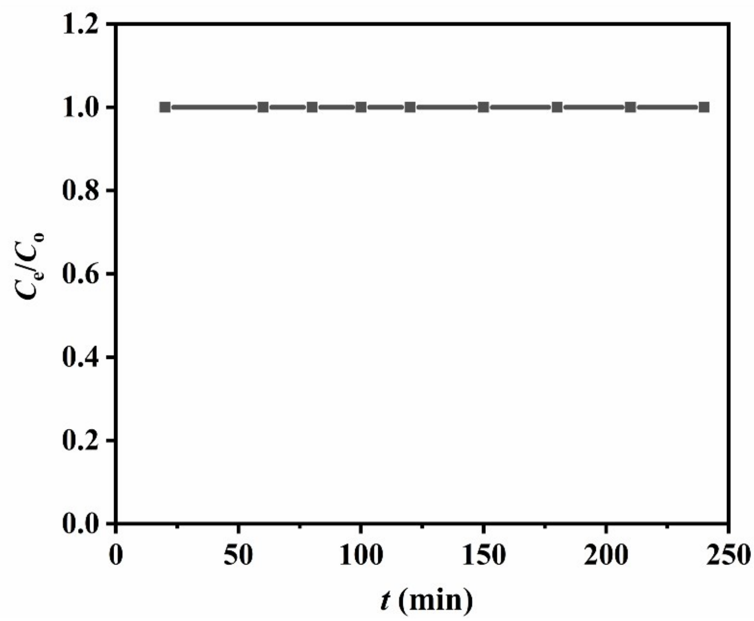

Figure S5 Blank experiment.

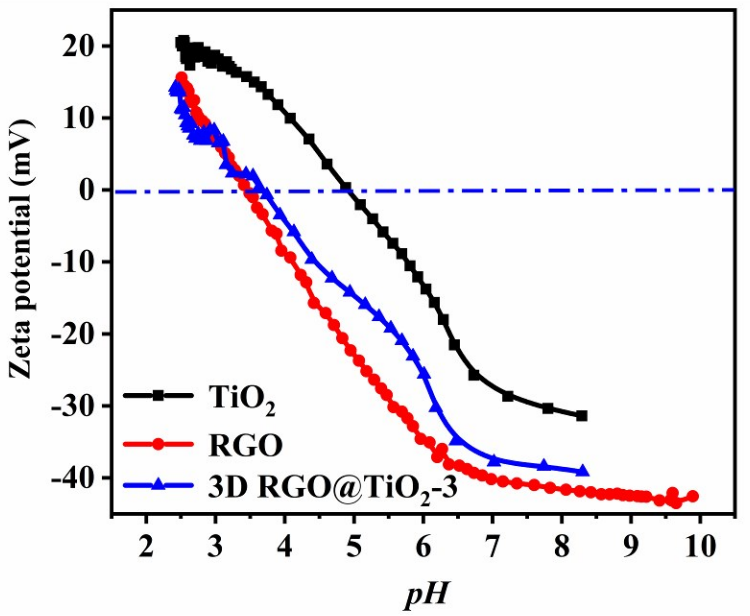

Figure S6 The zeta potential of samples.

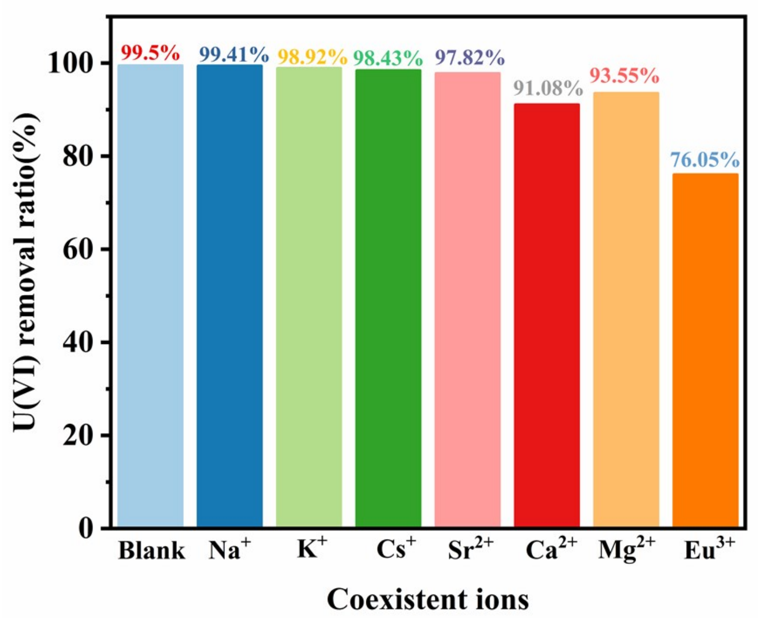

Figure S7 Effect of coexisting ions ($C_o \approx 50$ ppm, pH = 6.0, $m/V = 0.1$ g·L^{-1}, Methanol = 5 vol%, $T = 298$ K and $C_{\mathrm{metal}} = 0.2$ mol·L^{-1})

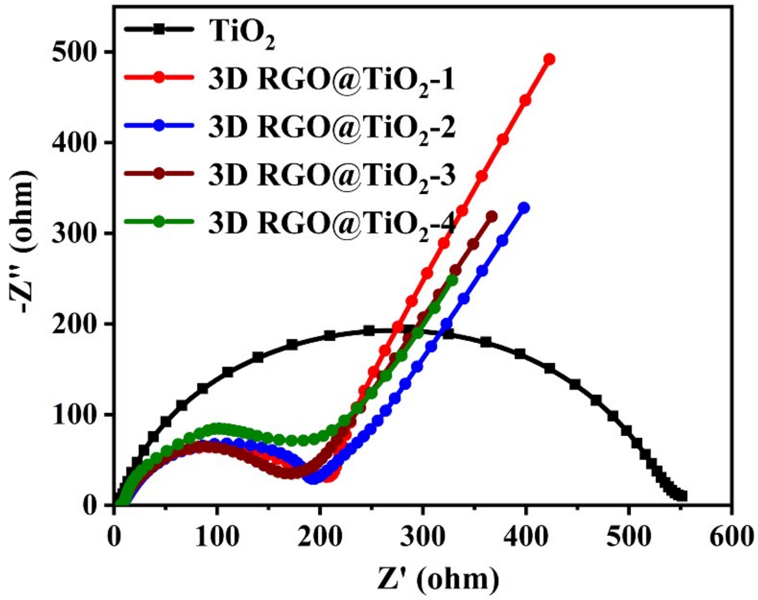

Figure S8 EIS Nyquisit plots of the prepared electrodes in 25 mmol·L^{-1} $K_3[Fe(CN)_6]$ of the H-TiO_2 and 3D RGO@TiO_2-x.

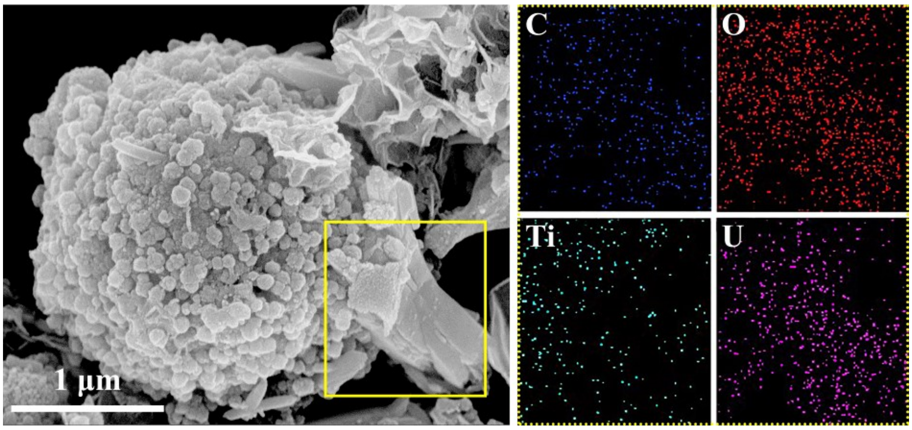

Figure S9 The SEM-mapping of 3D RGO@TiO_2-3 after U(VI) photoreduction.

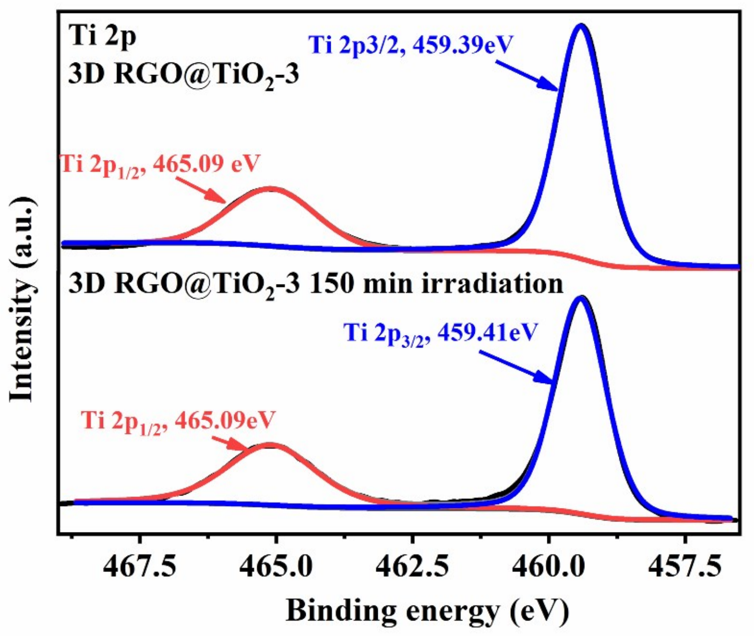

Figure S10 Ti 2p in of 3D RGO@TiO_2-3 and 3D RGO@TiO_2-3 photocatalytic reduction reaction alone.

Table S1 S_{BET}, V_t and D_A of the H-TiO$_2$ and 3D RGO@TiO$_2$-3

Catalysts	S_{BET}[a](m^2·g^{-1})	V_t[b](cm^3·g^{-1})	D_A[c](nm)
H-TiO$_2$	83.96	0.23	12.32
3D RGO@TiO$_2$-3	126.09	0.48	15.16

[a] BET specific surface area; [b] BET pore volume; [c] average pore diameters

Table S2 kinetic parameters of RGO and 3D RGO@TiO$_2$-x

Photocatalysts	RGO	3D RGO@TiO$_2$-1	3D RGO@TiO$_2$-2	3D RGO@TiO$_2$-3	3D RGO@TiO$_2$-4
K(min^{-1})	0.00754	0.00932	0.02300	0.03752	0.01698
R^2	0.99	0.99	0.96	0.92	0.91

Table S3 Fitting of the time-resolved PL spectra of the catalysts the nominal charge diffusion lengths

Catalysts	τ[a] (ns)	β[b]	^{L}H-TiO$_2$[c] (nm)	^{L} H-TiO$_2$[d] (nm)
TiO$_2$	7.44	1.10	16.37	8.97
3D RGO@TiO$_2$-1	7.60	0.94	16.55	9.07
3D RGO@TiO$_2$-2	10.93	1.02	19.84	10.87
3D RGO@TiO$_2$-3	11.29	1.06	20.17	11.05
3D RGO@TiO$_2$-4	9.87	1.08	18.86	10.33